Fiber Aided Wireless Network Architecture

Siddharth Ray, Muriel Médard, *Fellow, IEEE,* and Lizhong Zheng, *Member, IEEE*

***Abstract*—We introduce the concept of a fiber aided wireless network architecture (FAWNA), which allows high-speed mobile connectivity by leveraging the speed of optical networks. Specifically, we consider a single-input, multiple-output (SIMO) FAWNA, which consists of a SIMO wireless channel interfaced with an optical fiber channel through wireless-optical interfaces. We propose a design where the received wireless signal at each interface is sampled and quantized before being sent over the fiber. The capacity of our scheme approaches the capacity of the architecture, exponentially with fiber capacity. We also show that for a given fiber capacity, there is an optimal operating wireless bandwidth and number of interfaces. We show that the optimal way to divide the fiber capacity among the interfaces is to ensure that each interface gets enough rate so that its noise is dominated by front end noise rather than by quantizer distortion. We also show that rather than dynamically change rate allocation based on channel state, a less complex, fixed rate allocation scheme can be adopted with very small loss in performance.**

***Index Terms*—BWC, DAS, Fi-Wi, RoF.**

I. Introduction

THERE is a considerable demand for increasingly high-speed communication networks with mobile connectivity. Traditionally, high-speed communication has been efficiently provided through wireline infrastructure, particularly based on optical fiber, where bandwidth is plentiful and inexpensive. However, such infrastructure does not support mobility. Instead, mobile communication is provided by wireless infrastructure, most typically over the radio spectrum. However, limited available spectrum and interference effects limit mobile communication to lower data rates. Wireless-over-fiber technology allows the design of communication networks that feature high-speed as well as mobility.

A key attraction of wireless-over-fiber technology is that it centralizes most of the transceiver functionality by transmitting the wireless signals in their modulated format over fiber and reduces the fielded access points to antennas with associated amplifiers and frequency converters. Standards-independent and multi-service operation is facilitated. At frequencies used for existing cellular systems (900 MHz and 1.8 GHz for GSM, 2 GHz for UMTS), semiconductor lasers, directly modulated with the data modulated RF signals, SMF, and wide bandwidth photodiodes are preferred for wireless-over-fiber systems. A major cost saving is becoming available in such links with the development of high-linearity uncooled laser diodes [17].

Manuscript received 1 June 2010; revised 1 December 2010.

S. Ray is with Fawna Inc., Sunnyvale, CA 94085, USA (e-mail: sray06@gmail.com).

M. Médard and L. Zheng are with the Massachusetts Institute of Technology, Cambridge, MA 02139, USA (e-mail: medard@mit.edu, lizhong@mit.edu).

Digital Object Identifier 10.1109/JSAC.2011.110615.

Strong growth in the use of IEEE 802.11 a/b/g wireless local area networks (WLAN) has led to the development of systems for the simultaneous transmission of multiple WLAN channels over a single wireless-over-fiber link [18], showing the wide dynamic-range capabilities available with modern directly modulated lasers. For in-building applications, there has been considerable interest in the passive pico-cell concept [19], in which the base station uses a combined detector/optical modulator, which is directly coupled to the antenna, so that no electrical amplification or other processing is required. Typically, a waveguide electro-absorption modulator is used as the detector/modulator. However, this leads to system penalties due to the polarization dependence of the modulator and the high optical insertion loss. A more recent approach uses a normal incidence Automated Fiber Pigtailing Machine (AFPM) to give polarization independence and a low optical insertion loss by direct coupling to single-mode optical fiber [20]. Multi-mode fiber, although forming by far the majority of the in-building installed fiber base, has seen restricted use for wireless-over-fiber applications, since its small bandwidth distance product (typically less than 500 MHz km) requires signal transmission at intermediate frequency (IF) with up/down conversion at each Antenna Unit (AU) [21]. Above the multi-mode fiber cutoff frequency, the transmission response is fairly uniform, but at a lower level, and it has been shown to be possible to use this frequency range for wireless-over-fiber transmission without down/up conversion [22]. Tonguz and Jung [9], [11] consider an architecture where a given area is divided into microcells. Each microcell has a base station consisting of a single antenna and a laser diode. The wireless signals directly modulate this laser diode. The base stations are connected to a central base station using a single-mode fiber and the signal from each microcell is detected separately by a p-i-n detector at the receiver of the central base station. References [13], [14], [15] consider designs which use heating, ventilation, and air conditioning (HVAC) ducts for communicating the radio frequency signals to and from the central base station.

To cater for growth in broadband, wireless-access application spectrum has been made available in the 28, 40, and 60 GHz bands. Here, single sideband techniques are preferred to overcome dispersion limits on propagation in standard Single Mode Fiber (SMF). At higher frequencies, where direct modulation or external modulators are not available, a wide variety of techniques have been investigated [23] - [29] to provide broadband wireless-over- fiber access while minimizing the fiber dispersion penalties resulting from the high carrier frequency.

We introduce the concept of a fiber aided wireless network architecture (FAWNA), which allows high-speed mobile con-

nectivity by leveraging the speed of optical networks. Optical networks have speeds typically in hundreds of Megabit/sec or several Gigabit/sec (Gigabit Ethernet, OC-48, OC-192, etc.). In the proposed architecture, the network coverage area is divided into zones such that an optical fiber "bus" passes through each zone. Connected to the end of the fiber is a bus controller/processor, which coordinates use of the fiber as well as connectivity to the outside world. Along the fiber are radio-optical converters (wireless-optical interfaces), which are access points consisting of simple antennas directly connected to the fiber. Each of these antennas harvest the energy from the wireless domain to acquire the full radio bandwidth in their local environment and place the associated waveform onto a subchannel of the fiber. Within the fiber, the harvested signals can be manipulated by the bus controller/processor and made available to all other antennas. In each zone, there may be one or more active wireless nodes. Wireless nodes communicate between one another, or to the outside world, by communicating to a nearby antenna. Thus any node in the network is at most two hops away from any other node, regardless of the size of the network. In general, each zone is generally covered by several antennas, and there may also be wired nodes connected directly to the fiber.

In the architecture we propose, in order to dramatically simplify the functionality required at the individual antennas and provide much greater flexibility in their placement, a single centralized bus controller manages the complete state of the fiber and the associated communication sessions, including all switching, routing, monitoring, tracking, and path establishment. For example, it determines which zones are assigned to which sub-channels, and keeps track of which wireless nodes are contained in which zones, and which wired nodes are connected directly to the fiber. It also keeps track of interactions with the outside network. Much of this information is maintained in dynamic tables which must be distributed or shared with network users.

This architecture has the potential to reduce dramatically the interference effects that limit scalability and the energy-consumption characteristics that limit battery life, in pure wireless infrastructures. A FAWNA uses the wireline infrastructure to provide a distributed means of aggressively harvesting energy from the wireless medium in areas where there is a rich, highly vascularized wireline infrastructure and distributing in an effective manner energy to the wireless domain by making use of the proximity of transmitters to reduce interference. Note that FAWNA falls under the Radio-over-fiber (RoF) class of technologies.

We consider a single-input, multiple-output (SIMO) fiber aided wireless network architecture. We will also refer to this as SIMO-FAWNA. Figure 1 shows such a link between two points A and B. The various quantities in the figure will be described in detail in section 2. In the two hop link, the first hop is over a wireless channel and the second, over a fiber optic channel. The links we consider are ones where the fiber optic channel capacity is larger than the wireless channel capacity.

The transmitter at A transmits information to intermediate wireless-optical interfaces over a wireless SIMO channel. The wireless-optical interfaces then relay this information to the destination, B, over a fiber optic channel. The end-to-end design is done to maximize the transmission rate from A to B. Since a FAWNA has a large number of wireless-optical interfaces, an important design objective is to keep the wireless-optical interface as simple as possible without sacrificing too much in performance.

Our problem has a similar setup, but a different objective than the CEO problem [10]. In the CEO problem, the rate-distortion tradeoff is analyzed for a given source that needs to be conveyed to the CEO through an asymptotically large number of agents. Rate-distortion theory, which uses infinite dimensional vector quantization, is used to analyze the problem. We instead compute the maximum end-to-end rate at which reliable communication is possible. In general, duality between the two problems doesn't exist. Unlike the CEO problem, the number of wireless-optical interfaces is finite and the rate (from interface to receiver B) per interface is high, owing to the fiber capacity's being large. Finite-dimensional, high resolution quantizers are used at the interfaces. A similar multi-antenna over RoF has also been proposed as part of FP7 FUTON [30]. However, FAWNA has a completely digital wireless-optical interface compared to FUTON. Due to this, FAWNA is able to ensure lower signal distortion at the interface which results in a higher end-to-end capacity. Also, the cost and implementation complexity of the wireless-optical interface is significantly reduced because of digitization.

A FAWNA is an example of a channel model where quantization is performed between the source/channel encoding and decoding operations. Another example is a communication system where the receiver quantizes the incoming signal prior to decoding (Receiver implementation using a digital signal processor). Our analysis extends to all such channel models.

Let us denote the capacities of the wireless and optical channels as $C_w(P, W, r)$ and C_f bits/sec, respectively, where, P is the average transmit power at A, W is the wireless transmission bandwidth and r is the number of wireless-optical interfaces. Since, as stated earlier, we consider links where $C_w(P, W, r) \leq C_f$, the capacity of a SIMO-FAWNA, $C_{\mathsf{SIMO}}(P, W, r, C_f)$, can be upper bounded as

$$C_{\mathsf{SIMO}}(P, W, r, C_f) < \min\left\{C_w(P, W, r), C_f\right\} = C_w(P, W, r) \text{ bits/sec} \quad (1)$$

One way of communicating over a SIMO-FAWNA is to decode and re-encode at the wireless-optical interface. This is typically the process in digital-over-fibre solutions, which have been investigated and deployed commercially, for instance based in Common Public Radio Interface (CPRI) or Open Base Station Architecture Initiative (OBSAI) technologies for 2G mobile networks, or LTE (under development for 3G/4G). A major drawback of the decode/re-encode scheme is significant loss in optimality because "soft" information in the wireless signal is completely lost by decoding at the wireless-optical interface. Hence, multiple antenna gain is lost. Moreover, decoding results in the wireless-optical interface's having high complexity and requires the interface to have knowledge of the transmitter code book.

We propose a design where the wireless signal at each wireless-optical interface is sampled and quantized using a

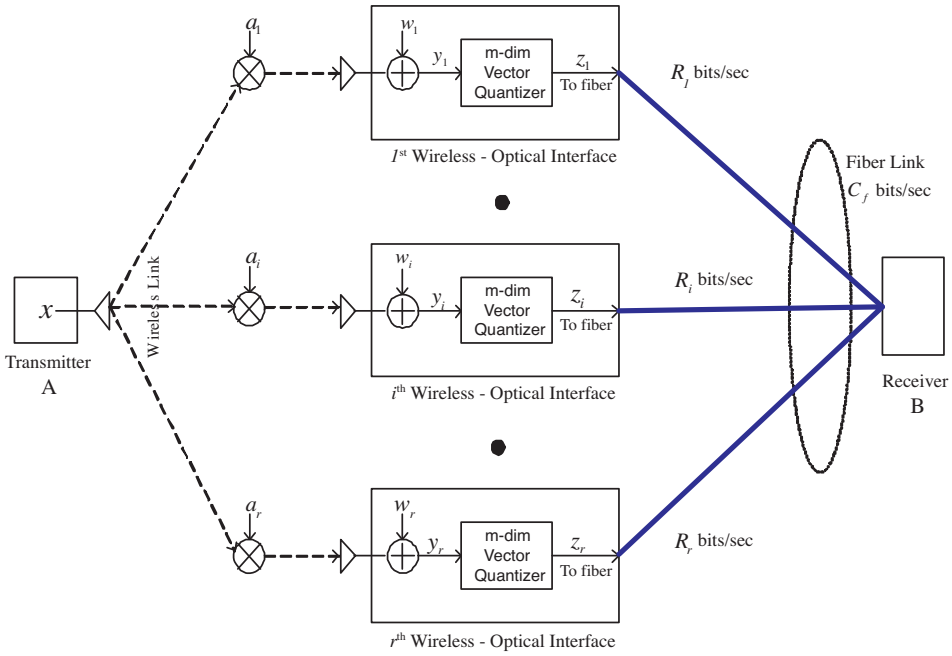

Fig. 1. A SIMO fiber aided wireless network architecture.

fixed-rate memoryless vector quantizer before being sent over the fiber. Hence, the interfaces use a forwarding scheme. Since lasers capable of analog modulation are expensive, it becomes commercially inviable to use them in a FAWNA that requires a large number of these. Hence, quantization is necessary for the implementation of a forwarding scheme in a FAWNA. The proposed design has quantization between end-to-end coding and decoding. Knowledge of the transmitter code book is not required at the wireless-optical interface. The loss in "soft" information due to quantization of the wireless signal, goes to 0 asymptotically with increase in fiber capacity. The interface has low complexity, is practically implementable, is extendable to FAWNAs with large number of transmitters and interfaces and, offers adaptability to variable rates, changing channel conditions and node positions.

We show that the capacity of our scheme approaches the upper bound (1), exponentially with fiber capacity. (We provide an example later on in the paper - Figure 5.) The proposed scheme is thus near-optimal since, the fiber capacity is larger than the wireless capacity. Low dimensional (or even scalar) quantization can be done at the interfaces without significant loss in performance. Not only does this result in low complexity, but also smaller (or no) buffers are required, thereby further simplifying the interface. Hui and Neuhoff [8] show that asymptotically optimal quantization can be implemented with complexity increasing at most polynomially with the rate. We establish the optimal way in which fiber capacity should be divided between the interfaces (interface rate allocation) and investigate robustness of FAWNA capacity with respect to it. We also analyze the loss from keeping rate allocation fixed (based on wireless channel statistics) rather than dynamically adjusting it according to channel state. For a SIMO-FAWNA with fixed fiber capacity, quantizer distortion as well as wireless capacity, $C_w(P, W, r)$, increases with wireless bandwidth and number of interfaces. The two competing effects result in the existence of an optimal operating wireless bandwidth and an optimal number of wireless-optical interfaces.

Let us establish notation that will be used in this paper. The bold type will be used to denote random quantities whereas normal type will be used to denote deterministic ones. Matrices will be denoted by capital letters and the scalar or vector components of matrices will be denoted using appropriate subscripts. Vectors will be represented by small letters with an arrow over them. All vectors are column vectors unless they have a ^{T} superscript. Scalars will be represented by small letters only. The superscript † will be used to denote the complex conjugate transpose. Unless specified otherwise, all logarithms in this chapter are to the base 2.

This paper is organized as follows: In section II, we describe our model and communication scheme. We analyze interface rate allocation and performance, in sections III and IV, respectively. We conclude in section V.

II. Model and Communication Scheme

There are r wireless-optical interfaces and each of them is equipped with a single antenna. The interfaces relay the wireless signals they receive from the transmitter, to the receiver at B, over an optical fiber. Communication over the fiber is interference free, which may be achieved, for example, using Time Division Multiple Access (TDMA) or Frequency Division Multiple Access (FDMA).

A. Wireless Channel

We use a linear model for the wireless channel between A and the wireless-optical interfaces:

$$\vec{\mathbf{y}} = \vec{\mathbf{a}}\mathbf{x} + \vec{\mathbf{w}}, \tag{2}$$

where, $\mathbf{x} \in \mathcal{C}, \vec{\mathbf{w}}, \vec{\mathbf{y}} \in \mathcal{C}^r$ are the channel input, additive noise and output, respectively. We assume ergodic block fading where, $\vec{\mathbf{a}} \in \mathcal{C}^r$ is the channel state that is random but fixed for the coherence time of the channel and changes independently from block to block. The channel state is independent of the channel input and the additive noise, and is perfectly known at the receiver at B but not at the transmitter and the wireless-optical interfaces. $\mathbf{a}_i$ denotes the channel gain from the transmitter to the i^{th} wireless-optical interface. The additive noise, $\vec{\mathbf{w}} \sim \mathcal{CN}(0, N_0 I_r)$, is independent of the channel input and $N_0/2$ is the double-sided white noise spectral density. (Note that this also includes distortion due to down-conversion.) The channel input, $\mathbf{x}$, satisfies the average power constraint, $E[|\mathbf{x}|^2] = P/W$, where, P and W are the average transmit power at A and wireless bandwidth, respectively. Hence, the ergodic wireless channel capacity is

$$C_w(P, W, r) = WE\left[\log\left(1 + \frac{\|\vec{\mathbf{a}}\|^2 P}{N_0 W}\right)\right], \tag{3}$$

and W symbols are transmitted over the wireless channel every second.

B. Fiber Optic Channel

The fiber optic channel between the wireless-optical interfaces and the receiver can reliably support a rate of C_f bits/sec. Communication over the fiber is interference free and the i^{th} interface communicates at a rate of R_i bits/sec with the receiver at B. Let us define the set of all rate vectors satisfying

$$\sum_{i=1}^{r} R_i = C_f,\ 0 < R_i \leq C_f,\ \text{for } i \in \{1, \ldots, r\}, \tag{4}$$

as $\mathcal{S}$. Fiber channel coding is performed at the wireless-optical interfaces to reliably achieve the rate vectors in $\mathcal{S}$. The signal received at the i^{th} wireless-optical interface is converted to baseband, sampled at the Nyquist rate of W complex samples/sec and quantized at a resolution of R_i/W bits/sample. It is assumed that there is no quantization jitter. These bits are then encoded before being sent over the fiber optic channel. The encoding at the wireless-optical interface needs to have the following key features: low implementation complexity, low latency, low overhead and, the ability to support high data rates. Since Radio Frequency (RF) samples are being sent over the fiber as opposed to IP packets, high reliability is not needed in the communication over the optical fiber since noise is dominated by the interface front end noise. Some examples of encoding techniques which can be used at the interface are Serial Rapid I/O (SRIO), PCI-Express, CPRI/OBSAI or Gigabit Ethernet. We assume error free communication over the fiber for all sum rates below fiber capacity. To keep the interfaces simple, source coding is not done at the interfaces. Since fiber capacity is large, the loss from not performing source coding is negligible. As an example, let us consider single carrier LTE operating over 20 MHz spectrum. The RF samples are typically quantized at 16 bits/complex sample (8 bits for I and 8 bits for Q). This results in a data rate of 20 Mhz x 16 bits/complex sample = 320 Mbps to be sent over the fiber. Current Gigabit Ethernet is able to support more than 1 Gbps over an optical fiber. Hence, the assumption that fiber transmission capacity greatly exceeds the bit rate required to transmit the encoded wireless signal, is a valid assumption. Note that the power consumption at each wireless-optical interface is around 200 - 500 mW. Overall, FAWNA has a similar power consumption as current wideband wireless over fiber systems (0.5 mW/m^2).

C. Communication Scheme

The input to the wireless channel, $\mathbf{x}$, is a zero mean circularly symmetric complex Gaussian random variable, $\mathbf{x} \sim \mathcal{CN}(0, P/W)$. Note that it is this input distribution that achieves the capacity of our wireless channel model. At each wireless-optical interface, the output from the antenna is first converted from passband to baseband and then sampled at the Nyquist rate of W complex samples/sec. The random variable, $\mathbf{y}_i$, represents the output from the sampler at the i^{th} interface. Fixed-rate memoryless m-dimensional vector quantization is performed on these samples at a rate of R_i/W bits/complex sample. The quantized complex samples are subsequently sent over the fiber after fiber channel coding and modulation. Thus, the fiber is required to support reliably a rate of R_i bits/sec from the i^{th} wireless-optical interface to the receiver at B.

The quantizer noise at the i^{th} interface, $\mathbf{q}_i$, is modelled as being additive. Hence, the two-hop channel between A and B can be modelled as:

$$\vec{\mathbf{z}} = \vec{\mathbf{a}}\mathbf{x} + \vec{\mathbf{w}} + \vec{\mathbf{q}}, \tag{5}$$

where, $\vec{\mathbf{q}} = [\mathbf{q}_1, \ldots, \mathbf{q}_r]^T$. The interfaces have noise from two sources, receiver front end (front end noise $\vec{\mathbf{w}}$) and distortion introduced by their quantizers ($\vec{\mathbf{q}}$). The quantizer at each interface is an optimal fixed rate memoryless m-dimensional high resolution vector quantizer. Hence, its distortion-rate function is given by the Zador-Gersho function [1], [4], [6]:

$$\begin{aligned} &E[|\mathbf{q}_i|^2] \\ &\quad = E[|\mathbf{y}_i|^2] M_m \beta_m 2^{-\frac{R_i}{W}} \\ &\quad = \left(N_0 + \frac{E\left[|\mathbf{a}_i|^2\right] P}{W}\right) M_m \beta_m 2^{-\frac{R_i}{W}}. \end{aligned} \tag{6}$$

M_m is the Gersho's constant, which is independent of the distribution of $\mathbf{y}_i$, and β_m is the Zador's factor, which depends on the distribution of $\mathbf{y}_i$. Since fiber channel capacity is large, the assumption that the quantizer is a high resolution one is valid. Hence, for all i, $R_i/W \gg 1$. Also, as this quantizer is an optimal fixed rate memoryless vector quantizer, references [2], [3], [4], [5], [7] show that the following hold: $E[\mathbf{q}_i] = 0$, $E[\mathbf{z}_i \mathbf{q}_i^*] = 0$ and $E[\mathbf{y}_i \mathbf{q}_i^*] = -E[|\mathbf{q}_i|^2]$. Therefore, $E[|\mathbf{z}_i|^2] = E[|\mathbf{y}_i|^2] - E[|\mathbf{q}_i|^2]$.

We denote the SIMO-FAWNA ergodic capacity using our scheme as $C_q(P, W, r, m, C_f)$. This can be expressed as

$$\begin{aligned} &C_q(P, W, r, m, C_f) \\ &\quad = WI(\mathbf{x}; \vec{\mathbf{z}} | \vec{\mathbf{a}}) \\ &\quad = WE\left[I(\mathbf{x}; \vec{\mathbf{z}} | \vec{\mathbf{a}} = \vec{a})\right] \\ &\quad = E\left[C_q^b(P, W, \vec{\mathbf{a}}, r, m, C_f)\right]. \end{aligned} \tag{7}$$

where, $C_q^b(P,W,\vec{a},r,m,C_f) \triangleq WI(\mathbf{x};\vec{\mathbf{z}}|\vec{a})$. Since our scheme is one among the possible schemes for a SIMO-FAWNA, we have

$$C_q(P,W,r,m,C_f) \leq C_{\mathsf{SIMO}}(P,W,r,C_f).$$

Hence, using (1), we obtain the following:

$$C_q(P,W,r,m,C_f) \leq C_{\mathsf{SIMO}}(P,W,r,C_f) < C_w(P,W,r). \quad (8)$$

We show later in this chapter that $C_q(P,W,r,m,C_f)$ approaches $C_w(P,W,r)$, exponentially with fiber capacity and hence, our scheme is near optimal. Observe that the wireless-optical interfaces have low complexity and do not require knowledge of the transmitter code book. They are extendable to FAWNAs with large number of transmitters and interfaces and offer adaptability to variable rates, changing channel conditions and node positions.

III. Interface Rate Allocation

In this section, we address two questions: First, how should rates be allocated to the interfaces in a coherence block and second, since channel state varies independently from block to block, is there significant loss in not computing the optimal rate allocation every block?

To answer the first question, consider the channel within a block interval. The channel state in this block takes the realization $\vec{a}$. We establish the following theorem:

Theorem 1: For any interface rate allocation, $\vec{R}$, we have

$$\begin{aligned} &C_q^b(P,W,\vec{a},r,m,C_f) \\ &\quad \geq W\log\left(\frac{1}{1-\frac{P}{N_0W}\vec{v}^\dagger M^{-1}\vec{v}}\right) \\ &\quad \triangleq C_{q,LB}^b(P,W,\vec{a},r,m,\vec{R}), \end{aligned} \quad (9)$$

where, $\vec{v}$ is specified for $i \in \{1,\ldots,r\}$ as

$$v_i = a_i(1 - M_m\beta_m 2^{-\frac{R_i}{W}}),$$

and M is specified for $i \in \{1,\ldots,r\}, j \in \{1,\ldots,r\}$ as

$$M_{ij} = \begin{cases} \frac{a_i a_j^* P}{N_0 W}\left(1 - M_m\beta_m 2^{-\frac{R_i}{W}}\right)\left(1 - M_m\beta_m 2^{-\frac{R_j}{W}}\right) & i \neq j, \\ \left(1 + \frac{|a_i|^2 P}{N_0 W}\right)\left(1 - M_m\beta_m 2^{-\frac{R_i}{W}}\right) & i = j. \end{cases}$$

Proof: See Appendix A. □

In the next section, we show that the supremum of the lower bound (9) over all rate vectors in $\mathcal{S}$, approaches $C_q^b(P,W,\vec{a},r,m,C_f)$, exponentially with fiber capacity. Hence, we consider this lower bound alone for finding the optimal interface rate allocation.

The optimal rate allocation for this block is given by

$$\vec{R}^*(\vec{a}) = \arg\max_{\vec{R}\in\mathcal{S}} \left[C_{q,LB}^b(P,W,\vec{a},r,m,\vec{R})\right]. \quad (10)$$

To understand optimal rate allocation, let us consider a SIMO-FAWNA with two interfaces[1], fiber capacity 200 Mbps, channel state $\vec{a} = [1\ \frac{1}{2}]^T$, $\frac{P}{N_0} = 100 \times 10^6$, $W = 5$ MHz and $M_m\beta_m = 1$. Since $R_2 = C_f - R_1$, it suffices to consider the capacity with respect to R_1 alone. The plot of $C_{q,LB}^b(P,W,\vec{a},r,m,\vec{R})$ with respect to R_1 is shown in figure 2.

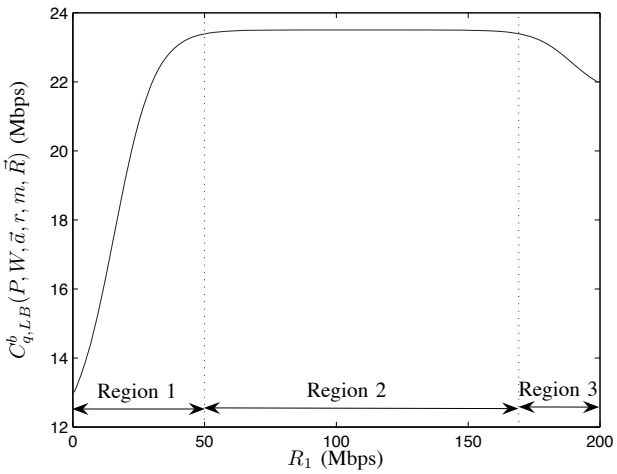

Fig. 2. Interface rate allocation for a two interface SIMO-FAWNA.

We can divide the plot into three regions. The first region is from 0 Mbps to 50 Mbps, where the first interface has low rate[2] and the second has high rate. Thus, noise at the first interface is quantizer distortion dominated whereas at the second interface is front end noise dominated. Hence, as we increase the rate for the first interface, the distortion at the first interface decreases and overall capacity increases. The reduction in rate at the second interface due to increase in R_1 has negligible effect on capacity since front end noise still dominates at the second interface.

The second region is from 50 Mbps to 170 Mbps. In this region, the rates for both interfaces are high enough for front end noise to dominate. Since quantizer distortion is low with respect to the front end noise at both interfaces, capacity is almost invariant to rate allocation. Observe that the capacity in this region is higher than that in the first and third regions and, the size of this region is much larger than that of the first and third.

The third region is from 170 Mbps to 200 Mbps and here, the first interface has high rate and the second has low rate. Therefore, noise at the first interface is front end noise dominated whereas at the second interface is quantizer distortion dominated. An increase in rate for the first interface results in decrease in rate for the second interface. This decrease in rate results in an increase in quantizer distortion at the second interface, which results in overall capacity decrease.

The channel gain at the first interface is higher than that at the second interface. Hence, compared to the second interface, the first interface requires more rate to bring its quantizer's distortion below the front end noise power. Also, reduction in quantizer distortion at the first interface results in higher capacity gains than reduction in quantizer distortion at the second interface. This can been seen from the asymmetric nature of the plot in figure 2 around $R_1 = 100$ Mbps.

[1]Even though we consider a two interface SIMO-FAWNA, results generalize to SIMO-FAWNAs with any number of interfaces.

[2]Whenever we mention "low rate", the rate considered is always high enough for the high resolution quantizer model to be valid.

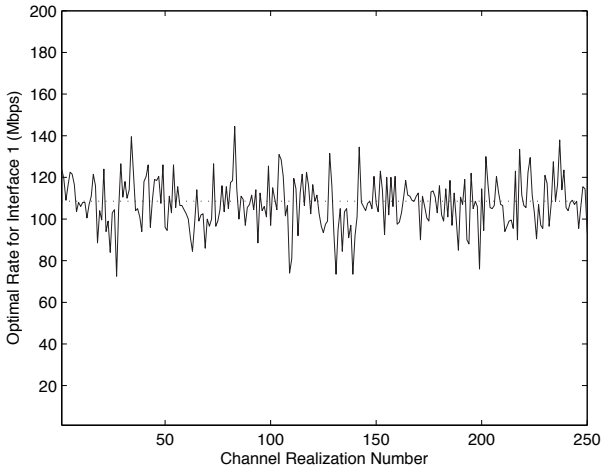

Fig. 3. Dynamic rate allocation.

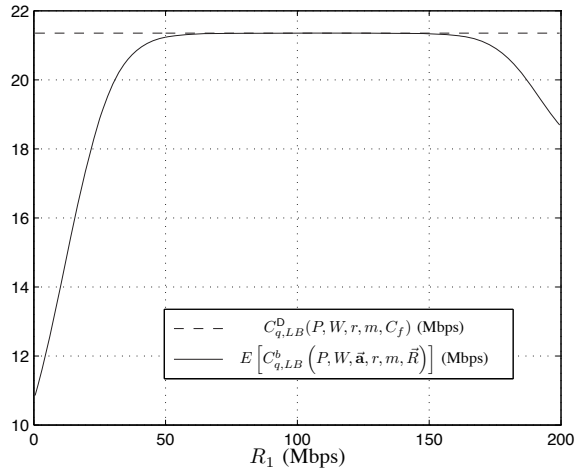

Fig. 4. Near-optimality of static rate allocation.

We see that the optimum interface rate allocation for a FAWNA is to ensure that each interface gets enough rate for it to lower its quantizer distortion to the point where its noise is front end noise dominated. Wireless-optical interfaces seeing higher channel gains require higher rates to bring down their quantizer distortion. After this requirement is met, FAWNA capacity is almost invariant to allocation of left over fiber capacity. This can be seen from the near flat capacity curve in the second region of the plot in figure 2. Thus, any interface rate allocation that ensures that noise at none of the wireless-optical interfaces is quantizer distortion dominated, is near optimal.

Since fiber capacity is large compared to the wireless capacity, the fraction of fiber capacity needed to bring down the distortion for the interfaces so that none of them is quantizer distortion limited, is small. Therefore, the set of interface rate vectors for which $C^{b}_{q,LB}(P,W,\vec{a},r,m,\vec{R})$ is near maximum, is large and there is considerable flexibility in allocating rates across the interfaces. Therefore, we see that large fiber capacity brings robustness to interface rate allocation in a FAWNA. For example, from figure 2, we see that even an equal rate allocation for the two interface SIMO-FAWNA is near-optimal.

We now address the second question posed at the beginning of this section: Since channel state changes independently from block to block, is there significant loss in not computing the optimal rate allocation every block? First, consider the case where interface rate allocation is dynamic, i.e., done in every block. The optimal rate allocation vector for the block is given by (10) and it depends on the channel realization (state). The ergodic capacity lower bound of a SIMO-FAWNA with dynamic rate allocation is given by

$$C^{\mathsf{D}}_{q,LB}(P,W,r,m,C_f) = E\left[C^{b}_{q,LB}\left(P,W,\vec{\mathbf{a}},r,m,\vec{R}^{*}(\vec{\mathbf{a}})\right)\right].$$

Consider the same two interface SIMO-FAWNA as in the previous question but with channel state $\vec{\mathbf{a}} = [\mathbf{h}_1 \ \frac{1}{2}\mathbf{h}_2]^T$, where $\mathbf{h}_1$ and $\mathbf{h}_2$ are i.i.d $\mathcal{CN}(0,1)$. For this channel, we compute $C^{\mathsf{D}}_{q,LB}(P,W,r,m,C_f) \sim 21.4$ Mbps. Figure 3 shows how the optimal rate for the first interface, R^{*}_{1}, changes with channel realization. Since the average channel gain at the first interface is larger than that at the second, the mean of the observations in the figure is above half the fiber capacity.

Dynamic rate allocation involves computation of the optimal rate allocation vector at the receiver at B and updating the interfaces with optimal values of rates, every coherence block. This considerably increases the complexity in a FAWNA. In order to simplify, we consider static rate allocation, i.e., interface rate allocation is computed based on wireless channel statistics and fixed forever. The interface rate allocation vector is chosen as one that maximizes the ergodic capacity lower bound:

$$\vec{R}^{*}_{\mathsf{S}} = \arg\max_{\vec{R}\in\mathcal{S}} E\left[C^{b}_{q,LB}\left(P,W,\vec{\mathbf{a}},r,m,\vec{R}\right)\right].$$

Hence, the ergodic capacity lower bound of a SIMO-FAWNA with static rate allocation is

$$C^{\mathsf{S}}_{q,LB}(P,W,r,m,C_f) = E\left[C^{b}_{q,LB}\left(P,W,\vec{\mathbf{a}},r,m,\vec{R}^{*}_{\mathsf{S}}\right)\right].$$

Note that this is sub-optimal to dynamic rate allocation:

$$C^{\mathsf{S}}_{q,LB}(P,W,r,m,C_f) \leq C^{\mathsf{D}}_{q,LB}(P,W,r,m,C_f) \leq C_q(P,W,r,m,C_f).$$

For the two interface SIMO-FAWNA, figure 4 shows how ergodic capacity changes with R_1. Since the ergodic capacity is the capacity averaged over channel realizations, this plot is similar to that in figure 2. From figure 4, we observe that $C^{\mathsf{S}}_{q,LB}(P,W,r,m,C_f) = 21.35$ Mbps and the near optimal rates for interface 1 are $R^{*}_{\mathsf{S},1} \sim [72,142]$ Mbps.

Note that the loss from static rate allocation is very small. Moreover, the set of static rate allocation vectors for which this loss is very small, is large. For this example, the loss is only 50 Kbps or 0.23% of capacity, and all rates from 72 Mbps to 142 Mbps are close to optimal for interface 1. Though the SIMO-FAWNA capacity is sensitive to quantizer distortion, large fiber capacity ensures that the interfaces always have enough rate so that they are never distortion limited over the typical set of channel realizations. This robustness of FAWNA capacity to interface rate allocation makes static rate allocation near-optimal. Observe from figure 4 that even equal rate allocation

is near-optimal. This near-optimality of static rate allocation translates to considerable reduction in FAWNA complexity. In general, when the fiber is heavily loaded either because it supports a large number of interfaces and/or a large number of frequency bands, it may not be possible to always ensure that all interfaces are not limited by quantizer distortion. In this scenario, the algorithms described in this section help in determining the optimal rate allocation among the interfaces.

IV. Effect of various parameters on performance

In this section, we analyze the effect of quantizer dimension, fiber capacity, transmit power, number of interfaces and wireless bandwidth on the performance of our scheme. To simplify analysis, we set the wireless channel gain $\vec{\mathbf{a}} = \mathbf{g} \cdot \vec{1}$, where, $\vec{1}$ is a r-dimensional column vector with all ones and $\mathbf{g}$ is a complex random variable. For this channel, all interfaces have the same instantaneous received power. Hence, an equal interface rate allocation is optimal: $\vec{R}^*(\mathbf{g} \cdot \vec{1}) = \vec{R}^*_{\mathsf{S}} = \frac{C_f}{r} \cdot \vec{1}$, and there is no loss from static interface rate allocation. Hence, $C^{\mathsf{S}}_{q,LB}(P, W, r, m, C_f) = C^{\mathsf{D}}_{q,LB}(P, W, r, m, C_f)$.

Since the ergodic capacity using dynamic rate allocation is the same as that using static rate allocation, we will remove the superscript to simplify notation and denote the ergodic capacity lower bound as $C_{q,LB}(P, W, r, m, C_f)$. Using Theorem 1, we can express this lower bound as

$$C_{q,LB}(P, W, r, m, C_f) = WE\left[\log\left(1 + \frac{r|\mathbf{g}|^2(1 - M_m\beta_m 2^{-\frac{C_f}{rW}})\frac{P}{N_0W}}{1 + \frac{|\mathbf{g}|^2 P M_m\beta_m 2^{-\frac{C_f}{rW}}}{N_0W}}\right)\right]. \quad (11)$$

We show in this section that the lower bound (11) approaches the upper bound $C_w(P, W, r)$ in (8), exponentially with fiber capacity. Hence, since the fiber capacity is large, the lower bound almost completely characterizes $C_q(P, W, r, m, C_f)$ and we consider this alone for analysis.

A. Effect of quantizer dimension

We now study the effect of quantizer dimension, m, on the performance of the proposed scheme. Since Gaussian signaling is used for the wireless channel, the input to the quantizer at the interface is a correlated Gaussian random vector. Zador's factor and Gersho's constant obey the following property: $M_\infty\beta_\infty \leq M_m\beta_m \leq M_1\beta_1 \leq M_1\beta_1^G$, where, β_1^G is the Zador's factor for an i.i.d Gaussian source and $\beta_1 \leq \beta_1^G$. $M_m\beta_m$ decreases with increase in m. Since $M_1 = \frac{1}{12}$, $M_\infty = \frac{1}{2\pi e}$, $\beta_1^G = 6\sqrt{3}\pi$ and $\beta_\infty = 2\pi e$, $1 \leq M_m\beta_m \leq \frac{\pi\sqrt{3}}{2}$. The lower bound corresponds to fixed rate infinite dimensional vector quantization whereas, the upper bound corresponds to fixed rate scalar quantization.

In (11), $\frac{r|\mathbf{g}|^2(1 - M_m\beta_m 2^{-\frac{C_f}{rW}})\frac{P}{N_0W}}{1 + \frac{|\mathbf{g}|^2 P M_m\beta_m 2^{-\frac{C_f}{rW}}}{N_0W}}$ decreases monotonically with increase in $M_m\beta_m$. Hence, $C_{q,LB}(P, W, r, m, C_f)$ increases with m and can be lower and upper bounded as

$$C_{q,LB}(P, W, r, 1, C_f) \leq C_{q,LB}(P, W, r, m, C_f) \leq C_{q,LB}(P, W, r, \infty, C_f),$$

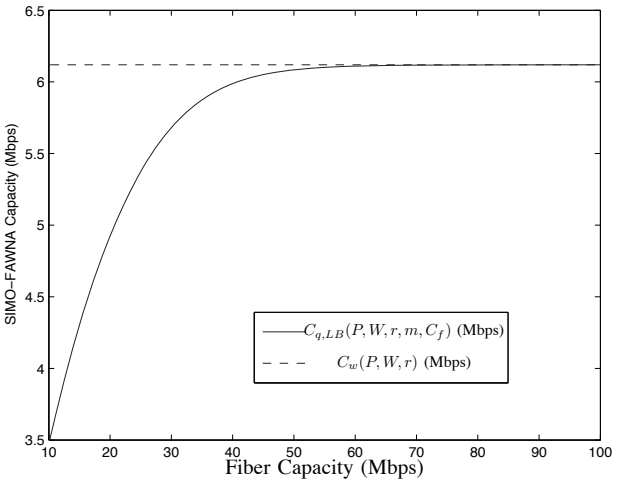

Fig. 5. Dependence of SIMO-FAWNA capacity on fiber capacity.

where, $C_{q,LB}(P, W, r, 1, C_f)$ and $C_{q,LB}(P, W, r, \infty, C_f)$ correspond to ergodic capacity lower bounds for fixed rate scalar and infinite dimensional vector quantization at the interfaces, respectively. Reduction in quantizer dimension reduces complexity at the interface but results in a capacity penalty. The maximum loss in capacity occurs when fixed rate scalar quantizers are used at the wireless-optical interfaces.

B. Effect of fiber capacity

We now analyze the effect of fiber capacity on the performance of a SIMO-FAWNA. Define $\Phi(C_f) \triangleq C_w(P, W, r) - C_{q,LB}(P, W, r, m, C_f)$. From (3, 11), we have

$$\Phi(C_f) = -WE\left[\log\left(1 - \frac{r|\mathbf{g}|^2\frac{P}{N_0W}(1 + \frac{|\mathbf{g}|^2P}{N_0W})M_m\beta_m 2^{-\frac{C_f}{rW}}}{1 + \frac{|\mathbf{g}|^2 P M_m\beta_m 2^{-\frac{C_f}{rW}}}{N_0W}}\right)\right].$$

Now,

$$\Phi(C_f) \leq -WE\left[\log\left(1 - \frac{r|\mathbf{g}|^2P}{N_0W}\left(1 + \frac{|\mathbf{g}|^2P}{N_0W}\right)M_m\beta_m 2^{-\frac{C_f}{rW}}\right)\right] = O(2^{-C_f}),$$

and

$$\Phi(C_f) \geq -WE\left[\log\left(1 - \frac{r|\mathbf{g}|^2\frac{P}{N_0W}(1 + \frac{|\mathbf{g}|^2P}{N_0W})M_m\beta_m 2^{-\frac{C_f}{rW}}}{1 + \frac{|\mathbf{g}|^2 P M_m\beta_m}{N_0W}}\right)\right] = \Omega(2^{-C_f}).$$

Hence, $\Phi(C_f) = \Theta(2^{-C_f})$ and $C_{q,LB}(P, W, r, m, C_f) = C_w(P, W, r) - \Theta(2^{-C_f})$. This implies that the ergodic capacity lower bound using the proposed scheme approaches the capacity upper bound (8), *exponentially* with fiber capacity. Also observe that $\Phi(\infty) = 0$. Note that though our scheme simply quantizes and forwards the wireless signals without source coding, we see that it is near optimal since the fiber capacity

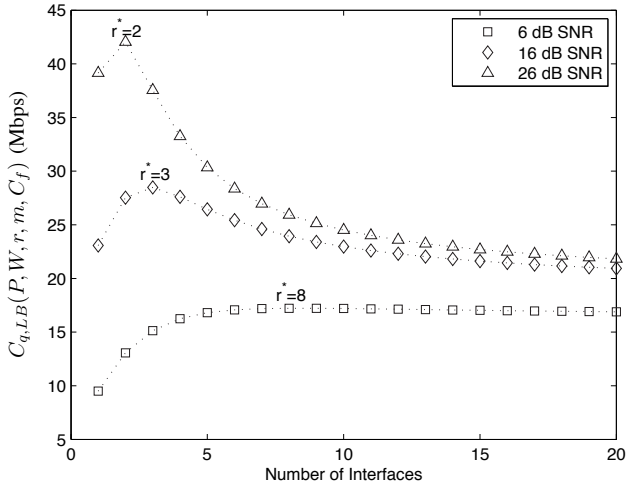

Fig. 6. Effect of the number of interfaces on $C_{q,LB}(P,W,r,m,C_f)$.

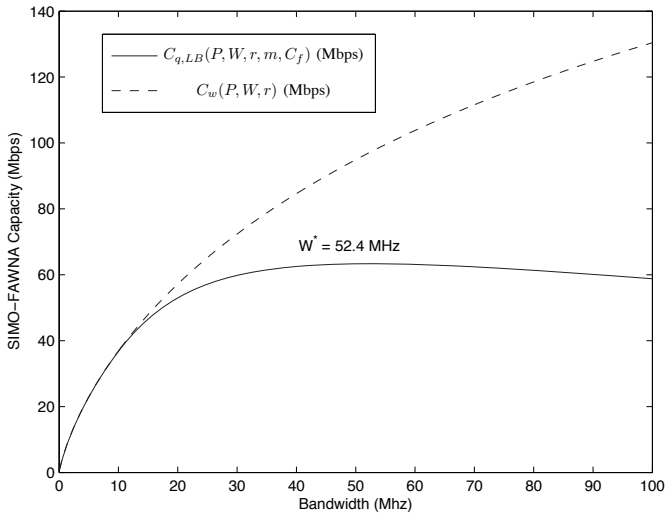

Fig. 7. Dependence of SIMO-FAWNA capacity on wireless bandwidth.

is much larger than the wireless capacity. This behavior is illustrated in figure 5. In the plot, we set $\mathbf{g} \sim \mathcal{CN}(0,1)$, $W = 1$ Mhz, $M_m\beta_m = 1$, $r = 5$ and $\frac{P}{N_0} = 25 \times 10^6$ sec^{-1}. Note that the fiber capacity required to achieve good performance is not large for an optical fiber, which has speeds in the order of Gigabit/sec.

C. Effect of transmit power

An increase in transmit power, P, leads to two competing effects. The first is increase in receive power at the interfaces, which increases capacity. The second is increase in quantizer distortion, which reduces capacity. The ergodic capacity lower bound of our scheme, $C_{q,LB}(P,W,r,m,C_f)$, increases monotonically with $\frac{r|\mathbf{g}|^2(1-M_m\beta_m 2^{-\frac{C_f}{rW}})\frac{P}{N_0W}}{1+\frac{|\mathbf{g}|^2PM_m\beta_m 2^{-\frac{C_f}{rW}}}{N_0W}}$, which in turn increases monotonically with P. Hence, the first effect always dominates and the ergodic capacity lower bound of our scheme *increases* with transmit power.

D. Effect of number of wireless-optical interfaces

Let us focus on the effect of the number of interfaces, r, on $C_{q,LB}(P,W,r,m,C_f)$. Since the quantization rate at the interface is never allowed to go below 1, the maximum number of interfaces possible is $r_{\max} = \lfloor \frac{C_f}{W} \rfloor$. Keeping all other variables fixed, the optimal number of interfaces, r^*, is given by

$$r^* = \arg \max_{r \in \{1,2,\ldots,r_{\max}\}} C_{q,LB}(P,W,r,m,C_f).$$

For fixed wireless bandwidth and fiber capacity, an increase in the number of interfaces leads to two competing effects. First, capacity increases owing to receive power gain from the additional interfaces. Second, quantizer distortion increases owing to additional interfaces sharing the same fiber, which results in capacity reduction. The quantization rate per symbol decays inversely with r. Hence, capacity doesn't increase monotonically with the number of antennas. Obtaining an analytical expression for r^* is difficult. However, r^* can easily be found by numerical techniques. Figure 6 is a plot of $C_{q,LB}(P,W,r,m,C_f)$ versus r for $\mathbf{g} \sim \mathcal{CN}(0,1)$, $W = 5$ Mhz, $M_m\beta_m = 1$, $C_f = 100$ Mbps. Note that, for this example, $r_{\max} = 20$. Plots are obtained for $\frac{P}{N_0} = 20 \times 10^6$ sec^{-1}, 200×10^6 sec^{-1} and 2000×10^6 sec^{-1}, which correspond to average interface signal-to-noise ratio (SNR) of 6 dB, 16 dB and 20 dB, respectively. The corresponding values of r^* are 8, 3 and 2, respectively. Observe that r^* decreases with increase in average interface SNR. This happens because, when average interface SNR is low, it becomes more important to gain power rather than to have fine quantization. On the other hand, when average interface SNR is high, the latter is more important. Hence, as average interface SNR decreases, r^* tends towards $r_{\max}$.

E. Effect of wireless bandwidth

We now analyze the effect of wireless bandwidth, W, on $C_{q,LB}(P,W,r,m,C_f)$. Since the quantization rate is never allowed to go below 1, the maximum possible bandwidth is C_f/r. For fixed fiber capacity and number of interfaces, the optimal bandwidth of operation, W^*, is given by

$$W^* = \arg \max_{W \in \left[0, \frac{C_f}{r}\right]} C_{q,LB}(P,W,r,m,C_f).$$

Since quantizer distortion as well as power efficiency increases with W, the behavior of the capacity lower bound with bandwidth is similar to that with the number of interfaces. Note that the quantization rate at each interface decays inversely with bandwidth. When the operating bandwidth is lowered from W^*, the capacity lower bound is lowered because the reduction in power efficiency is more than the reduction in quantizer distortion. On the other hand, when the operating bandwidth is increased from W^*, the loss in capacity from increased quantizer distortion is more than the capacity gain from increased power efficiency.

The optimal bandwidth, W^*, can be found by numerical techniques. Figure 7 shows the plot of the capacity lower

bound and $C_w(P,W,r)$, for $\mathbf{g} \sim \mathcal{CN}(0,1)$, $C_f = 200$ Mbps, $M_m\beta_m = 1$, $r = 2$ and $\frac{P}{N_0} = 100 \times 10^6$ sec^{-1}. The optimal bandwidth for this case is $W^* = 52.4$ Mhz.

V. Conclusion

In this paper, we study a SIMO-FAWNA from a capacity view point and propose a near-optimal design. We show that an optimal interface rate allocation is one which ensures that each interface gets enough rate so that its noise is dominated by front end noise rather than quantizer distortion. Capacity is almost invariant to the way in which left over fiber capacity is allocated. Hence, large fiber capacity ensures robustness of SIMO-FAWNA capacity to interface rate allocation. This robustness has an important implication on design, rather than dynamically change interface rate allocation based on channel state, a fixed rate allocation scheme can be adopted with very small loss in capacity. This results in considerable reduction in system complexity. We also show that for a given fiber capacity, there is an optimal operating wireless bandwidth and an optimal number of wireless-optical interfaces. The wireless-optical interfaces have low complexity and do not require knowledge of the transmitter code book. The design also has extendability to FAWNAs with large number of transmitters and interfaces and, offers adaptability to variable rates, changing channel conditions and node positions.

Future research may consider FAWNAs with multiple transmitters (with 1 or more antennas) and examine the performance of various multiple access schemes. For the multiple transmitters scenario, interference reduction and tradeoff between the various system parameters are interesting topics for study. Experimental demonstration to show the proof of concept is also another topic for future work.

Appendix A
Proof of Theorem 1

The channel state realization is $\vec{\mathbf{a}} = \vec{a}$. Consider another channel which differs from our model, (5), in only the quantization noise distribution. For this channel

$$\vec{\mathbf{z}}^G = \vec{a}\mathbf{x} + \vec{\mathbf{w}} + \vec{\mathbf{q}}^G,$$
$$\mathbf{q}_i^G \sim \mathcal{C}N(0, E[|\mathbf{q}_i|^2]), \quad i \in \{1,\ldots,r\}, \tag{12}$$

the quantization noise is jointly Gaussian with the input $\mathbf{x}$ and the following are satisfied:

$$E[\mathbf{z}_i^G \mathbf{q}_i^{G*}] = E[\mathbf{z}_i \mathbf{q}_i^*] = 0, \tag{13}$$
$$E[\mathbf{y}_i \mathbf{q}_i^{G*}] = E[\mathbf{y}_i \mathbf{q}_i^*] = -E[|\mathbf{q}_i|^2]. \tag{14}$$

Given the channel realization $\vec{a}$, since $\vec{\mathbf{q}}^G$ is jointly Gaussian with $\mathbf{x}$, $\vec{\mathbf{z}}^G$ is also jointly Gaussian with $\mathbf{x}$. References [12], [16] show that noise that is jointly Gaussian with the input, minimizes mutual information. Hence, we obtain the following bound:

$$I(\mathbf{x}; \vec{\mathbf{z}}^G | \vec{a}) \le I(\mathbf{x}; \vec{\mathbf{z}} | \vec{a}). \tag{15}$$

Let $\hat{\mathbf{x}}_{llse}(\vec{\mathbf{z}}^G)$ be the linear least-squares error (LLSE) estimate of $\mathbf{x}$ from $\vec{\mathbf{z}}^G$ and $\mathbf{e}_{llse}$, the corresponding estimation error. Hence, $\mathbf{x}$ can be expressed as $\mathbf{x} = \hat{\mathbf{x}}_{llse}(\vec{\mathbf{z}}^G) + \mathbf{e}_{llse}$. Since $\mathbf{x}$ and $\vec{\mathbf{z}}^G$ are jointly Gaussian, minimum mean-squares estimation (MMSE) is the same as LLSE estimation, and the estimation error is Gaussian and independent of the estimate. The variance of the estimation error is denoted as $\lambda_{llse} = E[|\mathbf{e}_{llse}|^2]$. We now compute the lower bound to the SIMO-FAWNA block capacity using our proposed scheme:

$$\frac{1}{W} C_q^b(P,W,\vec{a},r,m,C_f) = I(\mathbf{x}; \vec{\mathbf{z}} | \vec{a})$$
$$\ge I(\mathbf{x}; \vec{\mathbf{z}}^G | \vec{a}) \tag{16}$$
$$= h(\mathbf{x}) - h(\mathbf{e}_{llse}) = \log\left(\frac{P}{\lambda_{llse} W}\right). \tag{17}$$

We use (15) to obtain the inequality in (16). In order to compute the lower bound (17), λ_{llse} needs to be computed. This can be expressed as:

$$\lambda_{llse} = E[|\mathbf{x}|^2] - E[\mathbf{x}\vec{\mathbf{z}}^{G\dagger}] \Lambda_{\vec{\mathbf{z}}^G}^{-1} E[\mathbf{x}^* \vec{\mathbf{z}}^G], \tag{18}$$

where, $\Lambda_{\vec{\mathbf{z}}^G}$ is the autocorrelation matrix of $\vec{\mathbf{z}}^G$.

From our channel and quantizer models, we have the following Markov chains for $i \in \{1,\ldots,r\}$, $j \in \{1,\ldots,r\}$, $i \ne j$:

$$\mathbf{x} \leftrightarrow \mathbf{y}_i \leftrightarrow \mathbf{q}_i^G, \tag{19}$$
$$\mathbf{y}_i \leftrightarrow \mathbf{x} \leftrightarrow \mathbf{q}_j^G, \tag{20}$$
$$\mathbf{q}_i^G \leftrightarrow \mathbf{x} \leftrightarrow \mathbf{q}_j^G. \tag{21}$$

Using the first Markov chain, (19), we obtain:

$$E[\mathbf{x}\mathbf{q}_i^{G*}]$$
$$= E_{\mathbf{y}_i}\left[E[\mathbf{x}\mathbf{q}_i^{G*}|\mathbf{y}_i]\right] = E_{\mathbf{y}_i}\left[E[\mathbf{x}|\mathbf{y}_i]E[\mathbf{q}_i^{G*}|\mathbf{y}_i]\right]$$
$$= E_{\mathbf{y}_i}\left[\frac{E[\mathbf{x}\mathbf{y}_i^*]}{E[|\mathbf{y}_i|^2]}\mathbf{y}_i E[\mathbf{q}_i^{G*}|\mathbf{y}_i]\right] \tag{22}$$
$$= \frac{E[\mathbf{x}\mathbf{y}_i^*]E[\mathbf{y}_i\mathbf{q}_i^{G*}]}{E[|\mathbf{y}_i|^2]} = -\frac{a_i^* P M_m \beta_m 2^{-\frac{R_i}{W}}}{W}. \tag{23}$$

Since $\mathbf{x}$ and $\mathbf{y}_i$ are jointly Gaussian random variables, we obtain (22). Equation (23) follows from the quantizer properties (6, 14), and our wireless channel model (2). Using the second Markov chain, (20), we obtain for $i \ne j$:

$$E[\mathbf{y}_i\mathbf{q}_j^{G*}] = E_{\mathbf{x}}\left[E[\mathbf{y}_i\mathbf{q}_j^{G*}|\mathbf{x}]\right] = E_{\mathbf{x}}\left[E[\mathbf{y}_i|\mathbf{x}]E[\mathbf{q}_j^{G*}|\mathbf{x}]\right]$$
$$= E_{\mathbf{x}}\left[\frac{E[\mathbf{x}^*\mathbf{y}_i]}{E[|\mathbf{x}|^2]}\mathbf{x}E[\mathbf{q}_j^{G*}|\mathbf{x}]\right] \tag{24}$$
$$= \frac{E[\mathbf{x}^*\mathbf{y}_i]E[\mathbf{x}\mathbf{q}_j^{G*}]}{E[|\mathbf{x}|^2]} = -\frac{a_i a_j^* P M_m \beta_m 2^{-\frac{R_j}{W}}}{W}. \tag{25}$$

Since $\mathbf{x}$ and $\mathbf{y}_i$ are jointly Gaussian random variables, we obtain (24). Equation (25) follows from (23), and our wireless channel model (2). The third Markov chain, (21), gives us for $i \ne j$:

$$E[\mathbf{q}_i^G\mathbf{q}_j^{G*}] = E_{\mathbf{x}}\left[E[\mathbf{q}_i^G\mathbf{q}_j^{G*}|\mathbf{x}]\right] = E_{\mathbf{x}}\left[E[\mathbf{q}_i^G|\mathbf{x}]E[\mathbf{q}_j^{G*}|\mathbf{x}]\right]$$
$$= E_{\mathbf{x}}\left[\frac{E[\mathbf{x}^*\mathbf{q}_i^G]}{E[|\mathbf{x}|^2]}\mathbf{x}E[\mathbf{q}_j^{G*}|\mathbf{x}]\right] \tag{26}$$
$$= \frac{E[\mathbf{x}^*\mathbf{q}_i^G]E[\mathbf{x}\mathbf{q}_j^{G*}]}{E[|\mathbf{x}|^2]} = \frac{a_i a_j^* P M_m^2 \beta_m^2 2^{-\frac{R_i+R_j}{W}}}{W}. \tag{27}$$

Since $\mathbf{x}$ and $\mathbf{q}_i^G$ are jointly Gaussian random variables, we obtain (26). We obtain (27) from (23) and our wireless channel model (2). From (2) and (23), we obtain:

$$E[\mathbf{x}\mathbf{z}_i^{G*}] = E[\mathbf{x}\mathbf{y}_i^*] + E[\mathbf{x}\mathbf{q}_i^{G*}] = \frac{Pa_i^*(1 - M_m\beta_m 2^{-\frac{R_i}{W}})}{W} \triangleq \frac{P}{W}v_i^*. \quad (28)$$

We now compute $\Lambda_{\tilde{\mathbf{z}}^G}$. From (6, 14), for $i \in \{1, \ldots, r\}$,

$$E[|\mathbf{z}_i^G|^2] = E[|\mathbf{y}_i|^2] + E[\mathbf{y}_i\mathbf{q}_i^{G*}] + E[\mathbf{y}_i^*\mathbf{q}_i^G] + E[|\mathbf{q}_i|^2] = E[|\mathbf{y}_i|^2](1 - M_m\beta_m 2^{-\frac{R_i}{W}}) = N_0\left(1 + \tfrac{|a_i|^2 P}{N_0 W}\right)\left(1 - M_m\beta_m 2^{-\frac{R_i}{W}}\right) \triangleq N_0 M_{ii}, \quad (29)$$

and for $i \in \{1, \ldots, r\}, j \in \{1, \ldots, r\}, i \neq j$

$$\begin{aligned} E[\mathbf{z}_i^G\mathbf{z}_j^{G*}] &= E[\mathbf{y}_i\mathbf{y}_j^*] + E[\mathbf{y}_i\mathbf{q}_j^{G*}] + E[\mathbf{y}_j^*\mathbf{q}_i^G] + E[\mathbf{q}_i^G\mathbf{q}_j^{G*}] \\ &= a_i a_j^* \frac{P}{W} - \frac{a_i a_j^* P M_m \beta_m 2^{-\frac{R_j}{W}}}{W} - \frac{a_i a_j^* P M_m \beta_m 2^{-\frac{R_i}{W}}}{W} + \frac{a_i a_j^* P M_m^2 \beta_m^2 2^{-\frac{R_i+R_j}{W}}}{W} \\ &= \frac{a_i a_j^* P}{W}\left(1 - M_m\beta_m 2^{-\frac{R_i}{W}}\right)\left(1 - M_m\beta_m 2^{-\frac{R_j}{W}}\right) \\ &\triangleq N_0 M_{ij}. \end{aligned} \quad (30)$$

Combining equations (17, 18, 28, 29, 30) completes the proof. □

REFERENCES

[1] P. L. Zador, "Development and evaluation of procedures for quantizing multivariate distributions", *Ph.D. Dissertation, Stanford University*, 1963.

[2] J. G. Dunn, "The performance of a class of n dimensional quantizers for a Gaussian source", *Columbia Symp. on Signal Transm. Processing*, Columbia University, NY 1965.

[3] J. A. Bucklew and N. C. Gallagher, Jr., "A note on optimum quantization", *IEEE Trans. Inf. Theory*, vol. IT-25, pp. 365-366, May 1979.

[4] A. Gersho, "Asymptotically optimal block quantization", *IEEE Trans. Inf. Theory*, vol. IT-25, pp. 373-380, Jul 1979.

[5] N. C. Gallagher and J. A. Bucklew, "Properties of minimum mean squared error block quantizers", *IEEE Trans. Inf. Theory*, vol. IT-28, pp. 105-107, Jan 1982.

[6] P. L. Zador, "Asymptotic quantization error of continuous signals and the quantization dimension", *IEEE Trans. Inf. Theory*, vol. IT-28, pp. 139-148, Mar 1982.

[7] A. Gersho and R. M. Gray, "Vector Quantization and Signal Compression", *Kluwer*, Boston, MA, 1992.

[8] D. Hui and D. L. Neuhoff, "On the complexity of scalar quantization", *ISIT 95*, p. 372.

[9] H. Jung and O. K. Tonguz, "Comparison of Fiber and Coaxial Link for Access Network in Microcellular PCS", *IEE Electronics Lett.*, vol. 32, no. 5, pp. 425-426, Feb 1996.

[10] T. Berger, Z. Zhang and H. Viswanathan, "The CEO Problem", *IEEE Trans. Inf. Theory*, vol. 42, pp. 887-902, May 1996.

[11] O. K. Tonguz and H. Jung, "Personal Communications Access Networks using Subcarrier Multiplexed Optical Links", *IEEE J. Lightwave Technol.*, vol. 14, no. 6, pp. 1400-1409, Jun 1996.

[12] M. Médard, "Capacity of Correlated Jamming Channels", *Thirty-fifth Annual Allerton Conference on Comunication, Control and Computing*, Allerton, Illinois, Sep 1997.

[13] D. Stancil, O. K. Tonguz, A. Xhafa, P. Nikitin, A. Cepni, and D. Brodtkorb, "High-speed Internet Access via HVAC Ducts: A New Approach", *Globecom 2001*, Nov 2001.

[14] P. Nikitin, D. D. Stancil, O. K. Tonguz, A. Cepni, A. Xhafa, and D. Brodtkorb, "Impulse Response Characteristics of the HVAC Duct Communication Channel", *IEEE Trans. Commun.*, vol. 51, no. 10, pp. 1736-1742, Oct 2003.

[15] O. K. Tonguz, D. D. Stancil, A. Xhafa, A. G. Cepni, P. Nikitin, and D. Brodtkorb, "A Simple Path Loss Prediction Model for HVAC Systems", *IEEE Trans. Vehicular Technology*, Jul 2004.

[16] A. Kashyap, T. Başar and R. Srikant, "Correlated Jamming on MIMO Gaussian Fading Channels", *IEEE Trans. Inf. Theory*, vol. 50, pp. 2119-2123, Sep 2004.

[17] J. D. Ingham et al., "Wide-frequency-range operation of a high linearity uncooled DFB laser for next-generation radio-over-fiber," in *Proc. IEEE/OSA OFC*, Atlanta, GA, 2003, pp. 754756.

[18] T. Niiho et al., "Multi-channel wireless LAN distributed antenna system based on radio-over-fiber techniques," in *Proc. IEEE LEOS Annu. Meeting*. Rio Grande, Puerto Rico, 2004, pp. 5758.

[19] D. Wake, D. Johansson, and D. G. Moodie, "Passive picocell A new concept in wireless network infrastructure, Electron. Lett., vol. 33, no. 5, pp. 404406, Feb. 1997.

[20] C. Liu et al., "Bi-directional transmission of broadband 5.2 GHz wireless signals over fiber using a multiple-quantum-well asymmetric FabryProt modulator/photodetector, in Proc. IEEE/OSA OFC, Atlanta, GA, 2003, pp. 738740.

[21] LG cell product description. [Online]. Available: http://www. lgcwireless.com/products/lgcell.html

[22] P. Hartmann et al., "Low-cost multimode fiber-based wireless LAN distribution system using uncooled directly modulated DFB laser diodes, in Proc. ECOC, Rimini, Italy, 2003, pp. 804805.

[23] H. Ogawa, D. Polifko, and S. Bamba, "Millimetre-wave fiber optic systems for personal radio communication, *IEEE Trans. Microw. Theory Tech.*, vol. 40, no. 12, pp. 22852292, Dec. 1992.

[24] H. Schmuck and R. Heidemann, "High capacity hybrid fiber-radio field experiments at 60 GHz, in *Proc. IEEE/IEICE MWP*, Kyoto, Japan, 1996, pp. 6568.

[25] K. Kitayama, "Fading-free transport of 60 GHz optical DSB signal in non-dispersion shifted fiber using chirped fiber grating, in *Proc. IEEE MWP*, Princeton, NJ, 1998, pp. 223226.

[26] J. J. OReilly, P. M. Lane, and M. H. Capstick, "Optical generation and delivery of modulated mm-waves for mobile communications, in *Analogue Optical Fiber Communications, B. Wilson*, Z. Ghassemlooy, and I. Darwazeh, Eds. London, U.K.: Inst. Electr. Eng., 1995, pp. 229256.

[27] G. H. Smith and D. Novak, "Broadband millimetre-wave (38 GHz) fiber-wireless transmission system using electrical and optical SSB modulation to overcome dispersion effects, *IEEE Photon. Techol. Lett.*, vol. 10, no. 1, pp. 141143, Jan. 1998.

[28] K. I. Kitayama, T. Kuri, H. Yokoyama, and M. Okuno, "60 GHz millimetre-wave generation and transport over OFDM fiber-optic networks, in *Proc. IEEE/IEICE MWP*, Kyoto, Japan, 1996, pp. 4952.

[29] R. P. Braun, G. Grosskopf, D. Rohde, and F. Schmidt, "Fiber optic millimetre-wave generation and bandwidth efficient data transmission for broadband mobile 1820 and 60 GHz band communications, in *Proc. IEEE MWP*, Essen, Germany, 1997, pp. 235238.

[30] FP7 FUTON. [Online].Available: ftp://ftp.cordis.europa.eu/pub/fp7/ict/docs /future-networks/projects-futon-080311-futon-conc-meet.pdf

Siddharth Ray is currently with Fawna Inc. From 2006 to 2010, he was with the Flarion Technologies and Corporate Research & Development divisions of Qualcomm Inc. Dr. Ray received the B. Tech degree in Electrical Engineering from the Indian Institute of Technology Madras, India, in 2002, and the M. S. and Ph. D degrees in Electrical Engineering and Computer Science from the Massachusetts Institute of Technology, USA, in 2003 and 2006, respectively. Dr. Ray's research interests are in wireless communication, information theory and networks.

Muriel Médard is a Professor in the Electrical Engineering and Computer Science at MIT. She was previously an Assistant Professor in the Electrical and Computer Engineering Department and a member of the Coordinated Science Laboratory at the University of Illinois Urbana-Champaign. From 1995 to 1998, she was a Staff Member at MIT Lincoln Laboratory in the Optical Communications and the Advanced Networking Groups. Professor Mdard received B.S. degrees in EECS and in Mathematics in 1989, a B.S. degree in Humanities in 1990, a M.S. degree in EE 1991, and a Sc D. degree in EE in 1995, all from the Massachusetts Institute of Technology (MIT), Cambridge. She has served as an Associate Editor for the Optical Communications and Networking Series of the IEEE Journal on Selected Areas in Communications, as an Associate Editor in Communications for the IEEE Transactions on Information Theory and as an Associate Editor for the OSA Journal of Optical Networking. She has served as a Guest Editor for the IEEE Journal of Lightwave Technology, the Joint special issue of the IEEE Transactions on Information Theory and the IEEE/ACM Transactions on Networking on Networking and Information Theory and the IEEE Transactions on Information Forensic and Security: Special Issue on Statistical Methods for Network Security and Forensics. She serves as an associate editor for the IEEE/OSA Journal of Lightwave Technology. She is a member of the Board of Governors of the IEEE Information Theory Society. She has served as TPC co-chair of ISIT, WiOpt and CONEXT. Professor Mdard's research interests are in the areas of network coding and reliable communications, particularly for optical and wireless networks. She was awarded the 2009 Communication Society and Information Theory Society Joint Paper Award for the paper: Tracey Ho, Muriel Medard, Rolf Kotter, David Karger, Michelle Effros Jun Shi, Ben Leong, "A Random Linear Network Coding Approach to Multicast", IEEE Transactions on Information Theory, vol. 52, no. 10, pp. 4413-4430, October 2006. She was awarded the 2009 William R. Bennett Prize in the Field of Communications Networking for the paper: Sachin Katti , Hariharan Rahul, Wenjun Hu, Dina Katabi, Muriel Medard, Jon Crowcroft, "XORs in the Air: Practical Wireless Network Coding", IEEE/ACM Transactions on Networking, Volume 16, Issue 3, June 2008, pp. 497 - 510. She was awarded the IEEE Leon K. Kirchmayer Prize Paper Award 2002 for her paper, The Effect Upon Channel Capacity in Wireless Communications of Perfect and Imperfect Knowledge of the Channel," IEEE Transactions on Information Theory, Volume 46 Issue 3, May 2000, Pages: 935-946. She was co- awarded the Best Paper Award for G. Weichenberg, V. Chan, M. Mdard, "Reliable Architectures for Networks Under Stress", Fourth International Workshop on the Design of Reliable Communication Networks (DRCN 2003), October 2003, Banff, Alberta, Canada. She received a NSF Career Award in 2001 and was co-winner 2004 Harold E. Edgerton Faculty Achievement Award, established in 1982 to honor junior faculty members "for distinction in research, teaching and service to the MIT community." In 2007 she was named a Gilbreth Lecturer by the National Academy of Engineering.

Lizhong Zheng received the B.S and M.S. degrees, in 1994 and 1997 respectively, from the Department of Electronic Engineering, Tsinghua University, China, , and the Ph.D. degree, in 2002, from the Department of Electrical Engineering and Computer Sciences, University of California, Berkeley. Since 2002, he has been working in the Department of Electrical Engineering and Computer Sciences, where he is currently an associate professor. His research interests include information theory, wireless communications and wireless networks. He received Eli Jury award from UC Berkeley in 2002, IEEE Information Theory Society Paper Award in 2003, and NSF CAREER award in 2004, and the AFOSR Young Investigator Award in 2007. He is currently an associate editor of IEEE transactions on Information Theory.